Microporous and Mesoporous Materials 127 (2010) 25–31

Contents lists available at ScienceDirect

Microporous and Mesoporous Materials

journal homepage: www.elsevier.com/locate/micromeso

Confirmation of NH species in the framework of nitrogen-incorporated ZSM-5 zeolite by experimental and theoretical studies

Guangjun Wu, Xin Wang, Yali Yang, Landong Li, Guichang Wang, Naijia Guan *

Key Lab of Functional Polymer Materials, Department of Materials Chemistry, College of Chemistry, Nankai University, Tianjin 300071, PR China

ARTICLE INFO

Article history:
Received 8 January 2009
Received in revised form 15 June 2009
Accepted 22 June 2009
Available online 24 June 2009

Keywords:
ZSM-5 zeolite
Nitridation
Substitution
NH species
IR simulation

ABSTRACT

Nitrogen-incorporated zeolites have drawn much attention as a new family of basic solid materials and N atoms are expected to be introduced into the frameworks of zeolites. In this study, nitrogen-incorporated ZSM-5 zeolites were prepared by temperature-programmed nitridation and their physicochemical properties were characterized by means of XRD, SEM and BET techniques. Combined a detailed IR characterization with a theoretical IR simulation, the bands relating to bridging Si–N(H)–Si groups at 1151 and 985 cm^{-1} were observed in the IR fingerprint region of nitrogen-incorporated zeolites. The results confirmed that N atoms have been introduced into the framework of ZSM-5 zeolites by nitridation to form basic –NH– species, which was also supported by results of ^{29}Si MAS NMR characterization. Furthermore, the basic catalytic properties of nitrogen-incorporated ZSM-5 zeolites were evaluated by Knoevenagel condensation of benzaldehyde and malononitrile and enhanced conversion of benzaldehyde was achieved.

1. Introduction

Zeolites are used widely in adsorption, separation and catalysis, due to their unique pore structure, outstanding thermal and hydrothermal stability, shape selectivity and capacity of concentrating reactants inside the pores [1]. Recently, a new family of zeolites called ZOL has been successfully synthesized by Yamamoto and co-workers [2–4]. ZOL refers to zeolites with organic group as lattice, namely organic moieties, such as $–CH_2–$ and –NH– groups incorporated into the framework of the zeolites (denoted as ZOL–C and ZOL–N, respectively). As a new family of hybrid zeolite materials, ZOL presents significant unique properties. Elanany et al. [5] theoretically demonstrated that ZOL with CHA topology has lower Brønsted acid strength than the full oxygen CHA zeolite and the acid strength decreases in the order H–CHA > ZOL–C > ZOL–N. Lesthaeghe et al. [6,7] and Zheng et al. [8] showed the possible applications (such as alkylammonium formation and ethene protonation) of ZOL–N materials as bifunctional acid–base catalysts due to the presences of basic –NH– group and Brønsted acid site in a single structure. Furthermore, Astala and Auerbach [9] testified that ZOL–N materials were strong Lewis bases suggesting novel applications in base catalysis.

As strong Lewis bases with potential applications in base catalysis, ZOL–N materials, viz. nitrogen-incorporated zeolites, have been paid more attention. Since the first nitrogen-incorporated sample NaY zeolite was reported [10], various nitrogen-incorporated zeolites have been prepared, such as ZSM-5 [11–13], SAPO-11 [14], SAPO-34 [15], beta [16], and B-SSZ-13 [17]. Meanwhile, a series of nitrogen-incorporated mesoporous materials, e.g. MCM-41 [18–20], MCM-48 [21], SBA-15 [22], have also been reported. Compared with ZOL–C materials synthesized by hydrothermal method (similar to the synthesis of conventional zeolites) [23], ZOL–N materials are prepared by post-treatment method of nitridation. In a typical preparation process, certain zeolite is employed as precursor and the precursor is then treated at elevated temperature in NH_3 flow for a period of time to introduce nitrogen atoms into the framework of zeolite by substituting oxygen atoms in the lattice. The as-synthesized ZOL–N materials not only preserved good structure with the parent materials but also presented weakened Brønsted acid strength during catalytic process [13]. Moreover, very good activity in base probe reaction of Knoevenagel reaction has been observed on ZOL–N materials [12,16].

Astala and Auerbach [9] have theoretically demonstrated that the possible incorporation of $–CH_2–$ and –NH– groups in high concentrations into the framework of zeolites with minimal strain, however, the key issue for ZOLs is whether organic groups are included in the crystalline framework or not [23]. Owing to the high crystallinity of zeolite, the content of N or C incorporated is usually very low, which results in the difficulty to characterize the organic groups in the lattice of ZOL. IR spectroscopy is a useful technique and normally used to characterize the NH groups in the crystalline

* Corresponding author. Tel./fax: +86 22 23500319.
E-mail address: guannj@nankai.edu.cn (N. Guan).

1387-1811/$ - see front matter © 2009 Elsevier Inc. All rights reserved.
doi:10.1016/j.micromeso.2009.06.025

framework. The peak at ~3400 cm^{-1} attributed to the stretching vibrations of NH from Si–NH–Si groups in the FTIR spectra is considered as the evidence to demonstrate the existence of NH groups in the lattice of zeolite [16]. However, to the best of our knowledge, no peaks corresponding to N species has been reported in the fingerprint region (i.e. the wavenumber range of 400–1600 cm^{-1}) of FTIR spectra of ZOL–N materials. So, detailed characterizations on the organic groups are required to confirm the incorporation of N species into the framework of ZOL materials as well as to understand the mechanism of nitridation process.

In this paper, ZOL–N materials with MFI topology, viz. nitrogen-incorporated ZSM-5 zeolites, were prepared by temperature-programmed nitridation. The physicochemical properties and N species in the framework of as-synthesized samples were characterized by XRD, BET, SEM, FTIR and ^{29}Si MAS NMR. The peaks assigned to N species in the lattice were firstly observed in the fingerprint region of FTIR spectra. Furthermore, a theoretical IR simulation was also performed to support the results of experimental IR characterizations. Finally, Knoevenagel condensation of benzaldehyde and malononitrile was used as a basic probe reaction to explore the basic catalytic performances of nitrogen-incorporated ZSM-5 zeolites.

2. Experimental and computational details

2.1. Sample preparation

Microporous ZSM-5 zeolites (Si/Al > 300, commercial product from Catalysts Factory of Nankai University) were used as precursor. Temperature-programmed nitridation was carried out in the temperature range of 973–1173 K in a quartz tube furnace with different heating rates at constant NH_3 flow. A typical nitridation condition was present as follows: temperature = 1073 K, duration = 8 h, NH_3 flow rate = 60 ml/min, heating rate = 5 K/min, and the initial sample mass = 2.0 g. After being treated for 8 h, the sample was cooled down to room temperature and then treated in a vacuum oven at 398 K for another 4 h to remove adsorbed NH_3. The nitridated samples were respectively denoted as NZ-973, NZ-1073, and NZ-1173 with the numbers indicating the nitridation temperatures.

2.2. Sample characterization

FTIR spectra were performed on pure samples without KBr dilution by a Bruker VECTOR 22 FT-IR spectrophotometer. The thickness of the subtransparent wafers is 0.5–1 mm.

Solid-state 29Si NMR experiments at room temperature were performed on a Varian InfinityPlus-400 spectrometer equipped with a 7 mm probe (MAS was set to 4.5 MHz). The instrument operated at 79.4 MHz and the 90° pulses were 3 s.

Total nitrogen content of as-synthesized samples was determined by CNH elemental analysis on an Elementar Vario EL analyzer.

Powder X-ray diffraction patterns were collected on a D/Max-2500 powder diffractometer (36 kV and 20 mA) using Cu K_α (λ = 1.54178 Å) radiation from 5° to 50° with a scan speed of 2θ = 4.0°/min.

SEM images were obtained for structural identification using a HITACHI S-3500N Scanning Electron Microscope.

BET specific surface area was obtained by nitrogen adsorption on a Micromeritics ASAP 2020 facility at 77 K (liquid nitrogen temperature) after outgassing the samples for 2 h under vacuum at 673 K.

The basic catalytic properties of nitridation samples were evaluated by Knoevenagel condensation. Benzaldehyde (4 mmol), malononitrile (4 mmol) and 10 ml of toluene were added into a round bottom flask which was equipped with a magnetic stirrer and a reflux condenser and immersed in a thermostatic oil bath. Once the mixture reached 353 K, 0.2 g catalyst was added into the flask. Small liquid samples of 0.4 μl were then periodically withdrawn from the reaction mixture with a syringe and analyzed in a GC-7890F gas chromatograph equipped with a FID and a 0.32 mm × 35 m FFAP capillary column.

2.3. Computational details

Cluster models are failed to describe the micropore zeolitic structure, the electrostatic contributions of zeolite framework, and the interaction between the reactive system and zeolite wall [24], however, no qualitative difference or alternative paths of chemical reactions were observed when studied by means of cluster and periodic DFT modeling [24,25]. Therefore, 8T cluster [26,27] (Fig. S1) was selected as the computational cluster models of qualitative IR simulation to support the experimental results. The coordination of the atoms in the zeolite model was taken from the crystal structure of ZSM-5 reported by Koningsveld et al. [28]. There are 26 distinct O atoms in the unit cell of ZSM-5 zeolite. Here, the distinct O_{24} atom was selected as the substituted site for N atom because it binds to two distinct Si_{12} atoms, as shown in Fig. 1. The distinct Si_{12} atoms are located at the intersection of the straight and sinusoidal channels, which is characteristic of ZSM-5 zeolites and allows significant interaction between the bridging hydroxyl and adsorbed molecules and thus being considered as catalytically active sites [26,27]. In the cluster, each peripheral O atom or N atom was saturated with H atoms. The terminal O–H bond length was fixed at 0.1 nm along the direction of the O–Si bond as determined from crystallographic data. DFT method was used to simulate the IR spectra of nitrogen-incorporated ZSM-5 cluster. All the calculations in this study were performed by using Gaussian 98 program [29] at B3LYP/6-31G level.

Geometry optimization is important in quantum chemical cluster calculations to obtain reliable results. Since the full optimization might lead to structures that do not resemble experimental zeolite geometry [30], the nitrogen-incorporated ZSM-5 cluster was partially optimized. During calculation of the nitrogen-incorporated ZSM-5 cluster, the inner atoms of $O_3Si–N(H)–SiO_3$ were relaxed while the other atoms were anchored to their ZSM-5 positions. Then the IR simulation was performed on the partially optimized nitrogen-incorporated ZSM-5 cluster.

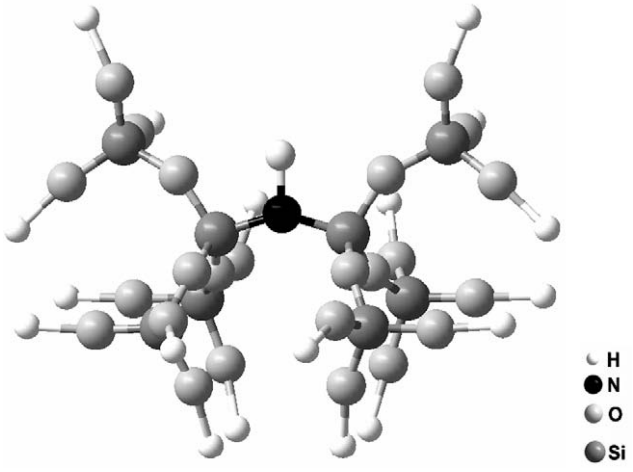

Fig. 1. Cluster model of nitrogen-incorporated ZSM-5 zeolite.

3. Results and discussion

3.1. Physicochemical properties of nitrogen-incorporated ZSM-5

Fig. 2 shows XRD patterns of ZSM-5 zeolites before and after nitridation at temperatures of 973, 1073, and 1173 K. Compared with the XRD pattern of parent ZSM-5 zeolites, the peak intensity of nitridated samples does not change obviously, indicating that nitridation under adopted conditions does not result in the structural destruction of nitridated ZSM-5 zeolites, a fact which can also be proved by SEM. SEM images of ZSM-5 and NZ-1073 in Fig. 3a, b show that the morphology of NZ-1073 is nearly the same as that of parent ZSM-5 zeolites. Moreover, the morphology of nitridated samples is also well-preserved with a longer nitridation time up to 20 h (Fig. 3c).

BET specific surface areas and pore volumes of ZSM-5 and nitridated sample NZ-1073 are summarized in Table 1. NZ-1073 still possesses large specific surface area and pore volume with respect to the parent ZSM-5 zeolite. It is thus indicated that the structure is well preserved after nitridation, in consistent with the results of XRD and SEM characterizations. Besides the conditions carried out not so extreme and the high thermal and hydrothermal stability of ZSM-5 zeolite, Narasimharao et al. [16] suggested that the ammonia atmosphere was probably an important factor in preserving the framework structure of zeolite during nitridation at high temperatures.

3.2. Characterizations of N species in the framework

During nitridation, two kinds of O atoms in ZSM-5 zeolite, i.e. terminal Si–OH group and bridge Si–O–Si groups, can be substituted by N atoms to form terminal Si–NH_2 groups and bridging Si–NH–Si groups, respectively. Thus the presence of –NH– species and Si–N(H)–Si species will confirm the N atoms in the framework of nitrogen-incorporated ZSM-5 zeolite. Different NH_x species on the nitridated samples can be efficiently distinguished by IR spectroscopy. Fig. 4 shows the FTIR spectra in the ranges from 3200 to 4000 cm^{-1} of as-synthesized samples which were treated under vacuum at 673 k for 1 h before IR measurements to diminish the contribution of adsorbed water. The band in the range of 3650–3750 cm^{-1} assigned to Si–OH groups (ν_{OH} vibrations), the band at 3611 cm^{-1} assigned to Si–OH–Al groups and the band at 3477 cm^{-1} assigned to adsorbed water [31,32] are observed in the spectrum of parent ZSM-5 zeolite. After nitridation, these bands change little in the spectrum of NZ-973 but drop sharply in the spectra of NZ-1073 and NZ-1173. Especially for bands at 3611 cm^{-1}, it almost disappears when nitridation temperature is over 1073 K. There maybe two reasons for this: one is that the O atom in Si–OH–Al group was substituted by N atoms and Si–NH–Al group was formed; another is that NH_3 molecule was protonated by Si–OH–Al group and $[Si–O–Al]^-NH_4^+$ group was formed. Meanwhile, a new band at 3406 cm^{-1} with a shoulder band at 3360 cm^{-1} are obviously observed when nitridation temperature is over 1073 K. According to relative literature [31], the band at 3406 cm^{-1} is assigned to stretching vibration of NH from Si–NH–

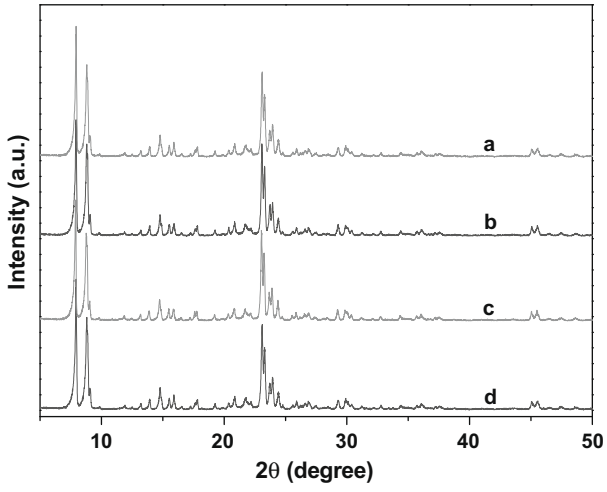

Fig. 2. XRD patterns of nitridated samples at different temperatures. (a) NZ-1173, (b) NZ-1073, (c) NZ-973, (d) parent ZSM-5.

Table 1
Textural properties of ZSM-5 zeolites before and after nitridation at 1073 K.

Samples	BET surface area (m^2/g)	Specific pore volume (cm^3/g)
ZSM-5	341	0.109
NZ-1073	318	0.111

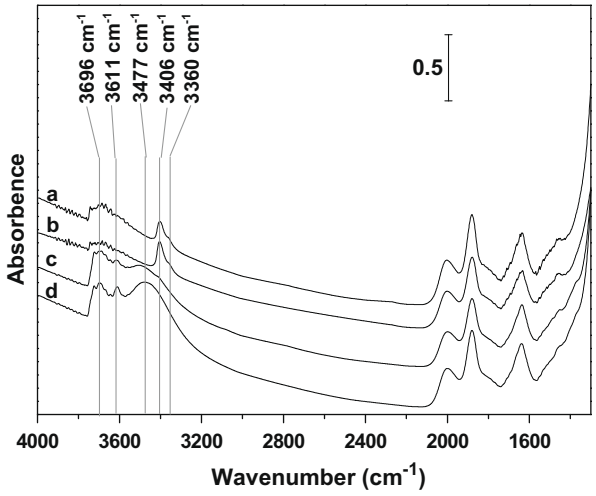

Fig. 4. FTIR spectra of nitridated samples treated under vacuum at 673 K for 1 h before IR measurements. (a) NZ-1173, (b) NZ-1073, (c) NZ-973, (d) parent ZSM-5.

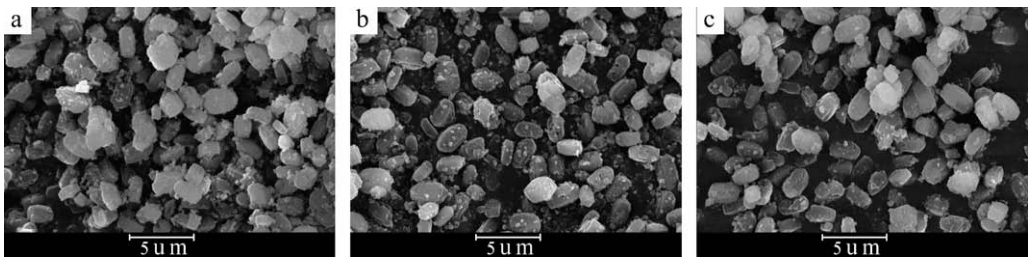

Fig. 3. SEM images of ZSM-5 zeolites before and after nitridation. (a) parent ZSM-5, (b) NZ-1073 nitridation for 8 h, (c) NZ-1073, nitridation for 20 h.

Si group and the shoulder band at 3360 cm^{-1} is assigned to stretching vibration of NH from Si–NH–Al group. It indicates that some O atoms in Si–OH–Al groups were substituted by N atoms and Si–NH–Al groups were formed and thus the band at 3611 cm^{-1} assigned to Si–OH–Al groups disappeared gradually. $-NH_2$ groups are also formed after nitridation by the reaction between the ≡Si–OH groups and NH_3 [16]. However, the band assigned to $-NH_2$ groups is absent in Fig. 4, which is observed in the spectra of all nitridated samples without pretreatment (See Fig. S1). It is indicated that the $-NH_2$ groups is unstable in nitridated samples and can be removed easily during pretreatment.

Fig. 5 presents the FTIR spectra in the IR fingerprint region, i.e. in the range from 1600 to 400 cm^{-1}, of nitridated samples without pretreatment. As shown in Fig. 5, the bands with low intensity at ~1402 cm^{-1} assigned to the stretching vibration of NH from adsorbed NH_4^+, i.e. NH_3 molecule attached to a Si–OH are observed in the spectra of all nitridated samples. A feature to note is that two shoulder bands appears at ~1151 cm^{-1} and ~985 cm^{-1} in the spectra of samples NZ-1073 (Fig. 5b) and NZ-1173 (Fig. 5a), which have not been reported in the nitrogen-incorporated zeolites before.

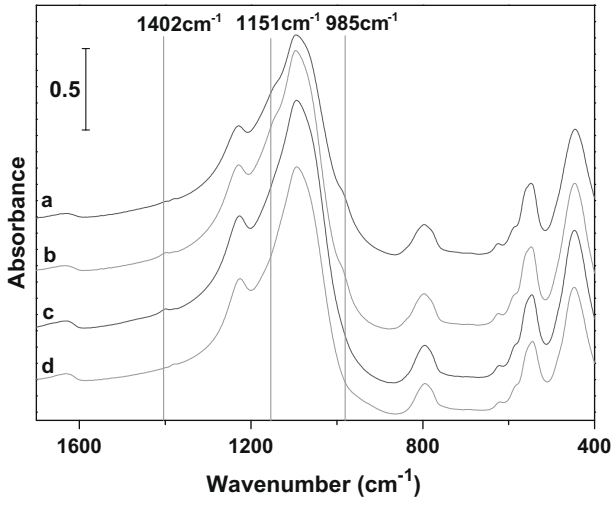

Fig. 5. FTIR spectra in the range from 1600 to 400 cm^{-1} of nitridated samples without pretreatment. (a) NZ-1173, (b) NZ-1073, (c) NZ-973, (d) parent ZSM-5.

In order to confirm the presence of IR bands in the fingerprint region, the second-derivative FTIR spectra are shown in Fig. 6. Besides the band at ~1399 cm^{-1} in Fig. 6a–c (corresponding to the band at ~1402 cm^{-1} in Fig. 5a–c), bands at ~1141 and ~977 cm^{-1} (corresponding to the bands at ~1151 and ~985 cm^{-1} in Fig. 5a and b) are more clearly observed, which begin to appear in the spectrum of NZ-973 (Fig. 6c) and develop rapidly in the spectra of NZ-1073 (Fig. 6b) and NZ-1173 (Fig. 6a). According to the FTIR study on silicon nitride [33–35] and nitrogen-incorporated mesoporous materials [20], the former is temporarily assigned to the bending vibrations of NH from Si–NH–Si (δ_{NH}) and the latter is assigned to the asymmetric stretching vibrations of Si–N(H)–Si ($\nu_{as\ Si-N-Si}$). The appearance of Si–N–Si group and –NH– species from bridging Si–NH–Si groups indicates that N atoms have been introduced into the framework of ZSM-5 zeolite by substituting O atoms.

^{29}Si MAS NMR is a useful technique in determining the chemical environment of Si atoms in nitrogen-incorporated microporous zeolites. As shown in Fig. 7, the dominating peak observed at −112 ppm is partially overlapped by the peak at approximately −115 ppm. These peaks are assigned to $Si*(OSi)_4$ in the framework of the ZSM-5 structure [36]. The ^{29}Si MAS NMR spectrum of ZSM-5 also exhibits a broad shoulder peak of the dominating peak in the range from −98 to −107 ppm, which is ascribed to $HOSi*(OSi)_3$ and/or $AlOSi*(OSi)_3$. After nitridation, a new peak at −92 ppm appears in the ^{29}Si MAS NMR spectrum of NZ-1073. According to the relevant literatures on silicon oxynitrides [37] and nitrogen-incorporated zeolites [12,20], this peak is ascribed to the SiO_3N, i.e. $HNSi*(OSi)_3$. The appearance of this peak indicates the formation of single $HNSi*(OSi)_3$ phase after nitridation and unambiguously confirms the presence of nitrogen in the framework of nitridated ZSM-5 zeolites.

However, no other peak is observed in the ^{29}Si MAS NMR spectra of NZ-973 and NZ-1073 besides the dominating peak at −112 and −115 ppm, the broad shoulder peak in range from −98 to −107 ppm and the peak at −92 ppm. Also, the peak at −92 ppm assigned to $HNSi*(OSi)_3$ is absent in the ^{29}Si MAS NMR spectrum of NZ-973, which suggests that the Si–NH–Si species is hardly formed at 973 K, being consistent with the results characterized by FTIR. However, both the FTIR spectra and CNH analysis (Table 2) suggest the presence of abundant $-NH_2$ group (i.e. $H_2NSi*(OSi)_3$) in NZ-973 and NZ-1073, so the broad peak in the range from −98 to −107 ppm in the spectra of NZ-973 and NZ-1073 is assigned to $H_2NSi(OSi)_3$ and/or $AlOSi(OSi)_3$ and/or $HOSi(OSi)_3$. Moreover, the

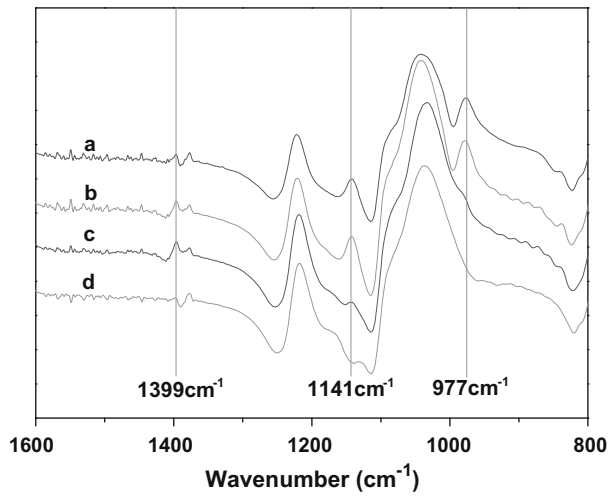

Fig. 6. Second-derivative FTIR spectra in the range from 1600 to 800 cm^{-1}. (a) NZ-1173, (b) NZ-1073, (c) NZ-973, (d) parent ZSM-5.

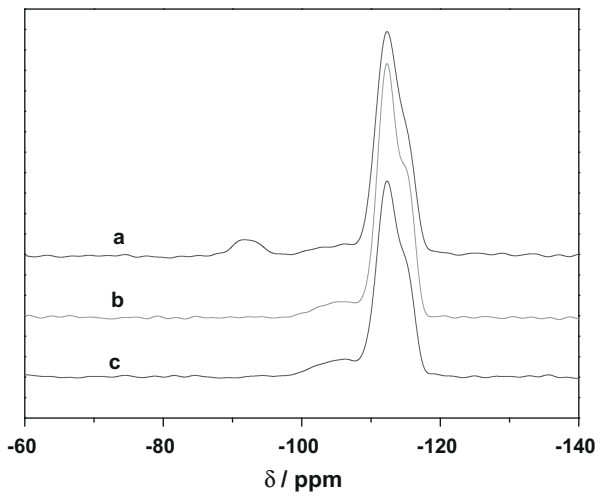

Fig. 7. ^{29}Si MAS NMR spectra of nitridated samples at different temperatures. (a) NZ-1073, (b) NZ-973, (c) parent ZSM-5.

Table 2
Nitrogen content of ZSM-5 zeolite before and after nitridation at temperatures of 973, 1073, and 1173 K.

Samples	ZSM-5	NZ-973	NZ-1073	NZ-1173
Nitrogen content (wt%)	–	1.10	1.15	1.49

intensity of broad shoulder peak in range from −98 to −107 ppm decreases in the ^{29}Si MAS NMR spectrum of NZ-1073, because of the reactions between ≡Si–OH and NH_3 and between ≡Si–NH_2 and ≡Si–OH [16]. This is consistent with the decrease of the intensity of band at ~3666 cm^{-1} attributed to the Si–OH in the FTIR spectrum of NZ-1073 (Figs. 4 and S1).

According to the FTIR and the ^{29}Si MAS NMR results, it is concluded that the NH species from bridging Si–NH–Si groups are formed at nitridation temperatures above 1073 K. The reason for this may be that the NH_3 molecules start decomposing apparently above ca. 1073 K [38,39].

3.3. IR simulation of nitrogen-incorporated ZSM-5 zeolite

The IR spectra of nitrogen-incorporated ZSM-5 zeolite were simulated by a DFT approach at B3LYP/6-31G(d) level to identify the IR bands observed in the experiments above. Scaling of the theoretical results needs to be considered since the simulated results are always not consistent with the experimental results [40]. Here, 0.9614 was used as the scaling factors at B3LYP/6-31G(d) level, which was demonstrated by Scott and Radom [40]. The optimized geometric parameters were present in Table S3 and the comparison of calculated result and experimental result were summarized in Table 3. In calculated result, four distinguishable vibrations relating to Si–O–Si groups in the framework of ZSM-5 zeolites were obtained. They are attributed to vibrations of SiO_4 tetrahedron at 1215, 1160, and 1100 cm^{-1} and bending vibration of O–Si–O at 464 cm^{-1}, corresponding to the bands at 1230, 1096, and 446 cm^{-1} in the FTIR spectra of ZSM-5 zeolite (Fig. 5). Compared the calculated results with experimental IR results, the absolute deviation percentage between them are smaller than 4.0%. Moreover, the non-scaled frequency in high-frequency and the scaled theoretical frequency in low-frequency completely consist with the experimental frequency, e.g. the bending vibration of O–Si–O groups (δ_{O-Si-O}) and the asymmetry vibration of SiO_4 tetrahedron. It is indicated that the calculated results are acceptable.

Six distinguishable vibrations relating to Si–NH–Si groups were obtained from the calculated results, as shown in Table 3. Fig. 8 shows the calculated vibration forms relating to Si–NH–Si groups, which are benefit to attribute the vibration. In high-frequency region, only asymmetric stretch vibration of NH species from bridging Si–NH–Si groups at 3474 cm^{-1} was obtained. In the fingerprint region, five vibrations relating to bridging Si–NH–Si groups at 1374, 1157, 1108, 502, and 484 cm^{-1} were obtained. According to the vibration directions of different atoms, the vibrations at 1374, 1157, 1108, 502, and 484 cm^{-1} are attributed to the bending vibration of NH species, complex vibrations of bending vibration of NH and symmetry vibration of O–Si–N, complex vibrations of bending vibration of NH and asymmetry vibration of O–Si–N, nonplanar bending vibration of NH from Si–NH–Si group, and bending vibration of Si–N–Si, respectively. Obviously, not all the theoretical vibrations can be observed in the experimental IR spectra, as the amount of –NH– species from Si–NH–Si groups is too low in comparison with the Si–O–Si groups and thus some of the bands are too weak and overlapped by dominating bands. However, it is necessary to point out that the vibration at 985 cm^{-1} observed in FTIR spectra of NZ-1073 and NZ-1173 and the symmetry vibration of Si–O–Si experimental observed at 800 cm^{-1} are absent in the calculated result. One of the reasons is that the calculated IR vibrations are multiplex and it is difficult to distinguish the attribution of every vibration. In any case, the band observed at 985 cm^{-1} is changed in accord with the change of band at 1151 cm^{-1}, which is confirmed to be related to Si–NH–Si groups. Consequently, the band at 985 cm^{-1} is related unambiguously to Si–NH–Si groups and the detailed assignments are still to be investigated.

Integrating the experimental results with computational results, it can be confirmed that –NH– species from bridging Si–NH–Si groups are formed after nitridation at elevated temperatures and N atoms have been introduced into the framework of zeolites by nitridation.

3.4. Catalytic performances

The Lewis basic sites will be formed on the surface of zeolites after nitridation and the surface basic property of nitrogen-incorporated zeolites will be improved, which has been demonstrated by experimental results [12,13,16] and theoretical results [5,9]. The Knoevenagel condensation is a base catalysis reaction under mild conditions and is often used as a basic probe reaction to evaluate the basic catalytic properties of nitrogen-incorporated zeolites [11,12,16] and mesoporous materials [19,21]. Here, the Knoevenagel condensation of benzaldehyde and malononitrile was used to explore the basic properties of as-synthesized samples. Fig. 9 shows the conversion of benzaldehyde on ZSM-5 zeolites before and after nitridation at different temperatures. The parent ZSM-5 zeolite possessed very low catalytic activity in Knovenagel condensation. In contrast, the nitridation samples showed considerable activity. After reaction for 8 h, the conversion on sample NZ-973 reached 55%, whereas the conversion on sample NZ-1073

Table 3
Comparison of theoretical frequencies and experimental frequencies.

Ascription	Theoretical frequencies (cm^{-1})		Experimental frequencies (cm^{-1})	Deviation percentage[a] (%)
	Calculated result	Scaled × 0.9614		
$\nu_{as\ -NH-}$	3474	3340	3410	1.84
δ_{-NH-}	1374	1321	–	–
$\nu_{SiO_4\ tetrahedron}$	1215	1168	1230	−1.23
$\nu_{SiO_4\ tetrahedron}$	1160	1115	–	–
$\delta + \nu_s$	1157	1112	1151	0.52
$\delta + \nu_{as}$	1108	1065	–	–
$\nu_{SiO_4\ tetrahedron}$	1100	1058	1096	0.36
Si–N–Si	–	–	985	–
$\nu_{s\ Si-O-Si}$	–	–	798	–
$\omega_{Si-NH-Si}$	502	483	–	–
$\delta_{Si-N-Si}$	484	465	–	–
δ_{Si-O}	464	446	446	3.88

[a] Deviation percentage = (1 − experimental frequency/theoretical frequency) × 100%.

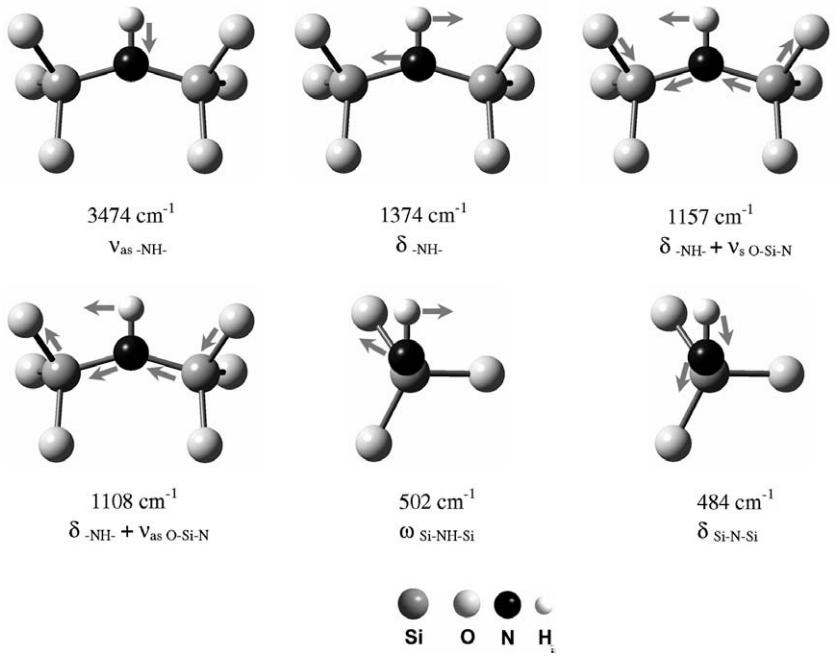

Fig. 8. Calculated vibrations relating to Si–N(H)–Si groups of nitrogen-incorporated ZSM-5 zeolite. ⟶: vibration direction of atoms.

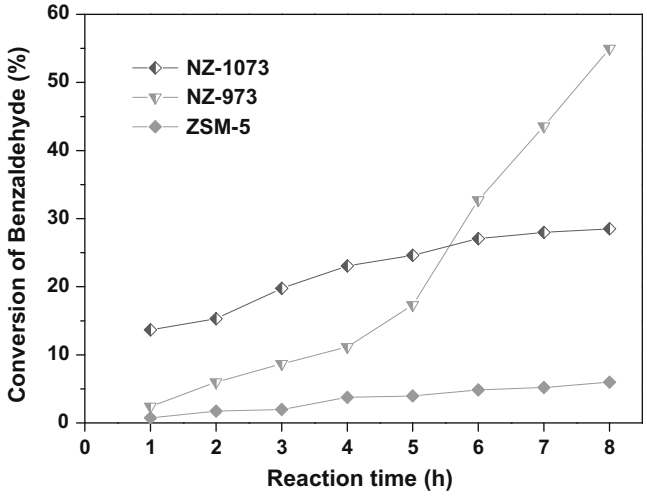

Fig. 9. Conversion of benzaldehyde in Knoevenagel condensation on ZSM-5 zeolites before and after nitridation at different temperatures.

reached 28%. This indicates that the surface basic property is improved by nitridation and nitrogen-incorporated zeolite can be used as a Lewis basic catalyst. It was also found that the selectivity to benzylidene malononitrile was close to 100% for all samples and no further reaction such as the Michael addition reaction, which involves the reaction of benzylidine malononitrile with another malononitrile molecule and requires stronger basic sites than Knoevenagel condensation [41], was detected.

Another feature to note is that the conversion on nitridated ZSM-5 zeolites did not depend in a simple manner on the nitrogen content of the samples. The initial conversion on sample NZ-1073 was higher than that on sample NZ-973. However, after reaction for 6 h, the conversion on sample NZ-973 became much higher than that on sample NZ-1073. It was suggested by Narasimharao et al. [16] that besides the nitrogen content, the nature of the framework nitrogen species also plays an important role in effecting the catalytic activity of benzaldehyde on nitrogen-incorporated zeolite and high catalytic activity for Knoevenagel condensations may requires both acidic (viz. Si–OH) and basic (viz. Si–NH_2) sites, which will be further studied in next work.

4. Conclusion

Nitrogen-incorporated microporous ZSM-5 zeolites can be synthesized by temperature-programmed nitridation while the structures can be well preserved after nitridated under certain conditions. The N atoms can be introduced into the framework of ZSM-5 zeolites to form basic –NH– species by nitridation, as confirmed by the observations of characteristic bands in the IR fingerprint region and the computational result. Consequently, the surface basic property of ZSM-5 zeolite is improved by nitridation and nitrogen-incorporated zeolite can be considered as a Lewis basic catalyst. However, the strengths and amount of the acid sites and basic sites need to be measured and the mechanism of nitridation is not clearly yet, which may give a direction to improve the nitridation method as well as the potential application of nitrogen-incorporated zeolites.

Acknowledgments

We gratefully acknowledge National Basic Research Program (No. 2009CB623502), National Natural Science Foundation of China (No. 20777039), and International S&T Cooperation Program of China (No. 2007DFA90720) for the financial support.

Appendix A. Supplementary data

Supplementary data associated with this article can be found, in the online version, at doi:10.1016/j.micromeso.2009.06.025.

References

[1] H. Hattori, Chem. Rev. 95 (1995) 537.
[2] K. Yamamoto, Y. Takahashi, T. Tatsumi, Stud. Surf. Sci. Catal. 135 (2001) 299.

[3] K. Yamamoto, Y. Sakata, Y. Nohara, Y. Takahashi, T. Tatsumi, Science 300 (2003) 470.
[4] Y. Yamamoto, Y. Nohara, Y. Domon, K. Takahashi, Y. Sakata, J. Plévert, T. Tatsumi, Chem. Mater. 17 (2005) 3913.
[5] M. Elanany, B.-L. Su, D.P. Vercauteren, J. Mol. Catal. A: Chem. 263 (2007) 195.
[6] D. Lesthaeghe, V. Van Speybroeck, M. Waroquier, J. Am. Chem. Soc. 126 (2004) 9162.
[7] D. Lesthaeghe, V. Van Speybroeck, G.B. Marin, M. Waroquier, J. Phys. Chem. B 109 (2005) 7952.
[8] A. Zheng, L. Wang, L. Chen, Y. Yue, C. Ye, X. Lu, F. Deng, Chem. Phys. Chem. 8 (2007) 231.
[9] R. Astala, S.M. Auerbach, J. Am. Chem. Soc. 126 (2004) 1843.
[10] G.T. Kerr, G.R. Shipman, J. Phys. Chem. 72 (1968) 3071.
[11] S. Ernst, M. Hartmann, S. Sauerbeck, T. Bonger, Appl. Catal. A: Gen. 200 (2000) 117.
[12] C. Zhang, Z. Xu, K. Wan, Q. Liu, Appl. Catal. A: Gen. 258 (2004) 55.
[13] X. Guan, N. Li, G. Wu, J. Chen, F. Zhang, N. Guan, J. Mol. Catal. A: Chem. 248 (2006) 220.
[14] J. Xiong, Y. Ding, H. Zhu, L. Yan, X. Liu, L. Lin, J. Phys. Chem. B 107 (2003) 1366.
[15] X. Guan, F. Zhang, G. Wu, N. Guan, Mater. Lett. 60 (2006) 3141.
[16] K. Narasimharao, M. Hartmann, H.H. Thiel, S. Ernst, Micropor. Mesopor. Mater. 90 (2006) 377.
[17] L. Regli, S. Bordiga, C. Busco, C. Prestipino, P. Ugliengo, A. Zecchina, C. Lamberti, J. Am. Chem. Soc. 129 (2007) 12131.
[18] J.E. Haskouri, S. Cabrera, F. Sapiña, J. Larorre, C. Guillem, A. Beltrán-Porter, D. Beltrán-Porter, M.D. Marcos, P. Amorós, Adv. Mater. 13 (2001) 192.
[19] Y. Xia, R. Mokaya, J. Mater. Chem. 14 (2004) 2507.
[20] C. Zhang, Q. Liu, Z. Xu, J. Non-Cryst. Solids 351 (2005) 1377.
[21] Y. Xia, R. Mokaya, Angew. Chem. Int. Ed. 42 (2003) 2639.
[22] N. Chino, T. Okubo, Micropor. Mesopor. Mater. 27 (2005) 15.
[23] K. Yamamoto, T. Tatsumi, Chem. Mater. 20 (2008) 972.
[24] X. Rozanska, X. Saintigny, R.A. van Santen, F. Hutschka, J. Catal. 202 (2001) 141.
[25] E.A. Pidko, R.A. van Santen, J. Phys. Chem. C 111 (2007) 2643.
[26] S.R. Lonsinger, A.K. Chakraborty, D.N. Theodorou, A.T. Bell, Catal. Lett. 11 (1991) 209.
[27] S.P. Yuan, J.G. Wang, Y.W. Li, S.Y. Peng, J. Mol. Catal. A: Chem. 178 (2002) 267.
[28] H. van Koningsveld, H. van Bekkum, J.C. Jansen, Acta. Cryst. B 43 (1987) 127.
[29] M.J. Frisch, G.W. Trucks, H.B. Schlegel, G.E. Scuseria, M.A. Robb, J.R. Cheeseman, V.G. Zakrzewski, J.A. Montgomery Jr., R.E. Stratmann, J.C. Burant, S. Dapprich, J.M. Millam, A.D. Daniels, K.N. Kudin, M.C. Strain, O. Farkas, J. Tomasi, V. Barone, M. Cossi, R. Cammi, B. Mennucci, C. Pomelli, C. Adamo, S. Clifford, J. Ochterski, G.A. Petersson, P.Y. Ayala, Q. Cui, K. Morokuma, D.K. Malick, A.D. Rabuck, K. Raghavachari, J.B. Foresman, J. Cioslowski, J.V. Ortiz, A.G. Baboul, B.B. Stefanov, G. Liu, A. Liashenko, P. Piskorz, I. Komaromi, R. Gomperts, R.L. Martin, D.J. Fox, T. Keith, M.A. Al-Laham, C.Y. Peng, A. Nanayakkara, C. Gonzalez, M. Challacombe, P.M.W. Gill, B. Johnson, W. Chen, M.W. Wong, J.L. Andres, C. Gonzalez, M. Head-Gordon, E.S. Replogle, J.A. Pople. Gaussian 98, Revision A.9, Gaussian, Inc., Pittsburgh, PA, 1998.
[30] J. Sauer, in: G. Pacchioni, P.S. Bagus, F. Parmigiani (Eds.), Cluster Models for Surface and Bulk Phenomena, Plenum Press, New York, 1992, p. 533.
[31] P. Fink, J. Datka, J. Chem. Soc., Faraday Trans. 1 (85) (1989) 3079.
[32] E. Astorino, J.B. Peri, R.J. Willey, G. Busca, J. Catal. 157 (1995) 482.
[33] G. Busca, V. Lorenzelli, G. Porcile, M.I. Baraton, P. Quintard, R. Marchand, Mater. Chem. Phys. 14 (1986) 123.
[34] D.L. Wood, E.M. Rabinovich, Appl. Spectrosc. 43 (1989) 263.
[35] I. Nowak, M. Ziolek, Catal. Today 118 (2006) 410.
[36] C.J.H. Jacobsen, C. Madsen, T.V.W. Janssens, H.J. Jakobsen, J. Skibsted, Micropor. Mesopor. Mater. 39 (2000) 393.
[37] C.J.H. Jacobsen, C. Madsen, J. Houzvicka, I. Schmidt, A. Carlsson, J. Am. Chem. Soc. 122 (2000) 7116.
[38] J. Soberg, R. Pompe, J. Am. Ceram. Soc. 75 (1992) 2189.
[39] R.V. Weeren, E.A. Leone, S. Curran, L.C. Klein, S.C. Danforth, J. Am. Ceram. Soc. 77 (1994) 2699.
[40] A.P. Scott, L.J. Radom, Phys. Chem. 100 (1996) 16502.
[41] M.J. Climent, A. Corma, R. Guil-Lopez, S. Iborra, Catal. Lett. 74 (2001) 161.